Oncology and Translational Medicine
DOI 10.1007/s10330-016-0210-0

June 2017, Vol. 3, No. 3, P116–P126

ORIGINAL ARTICLE

The role of the HGF/c-Met signaling pathway in crizotinib-induced apoptosis in lung cancer with c-Met amplification*

Shaozhang Zhou[1], Zhixin Dong (Co-first author)[2], Jinyi Lv[2], Aiping Zeng[1], Huilin Wang[1], Ruiling Ning[1], Xiangqun Song[1] (✉)

[1] The Second Department of Chemotherapy, The Affiliated Tumor Hospital, Guangxi Medical University, Guangxi 530021, China
[2] Guangxi Medical University Graduate School, Guangxi 530021, China

Abstract

Objective This study aimed to study the role of the HGF/c-Met signaling pathway in crizotinib-induced apoptosis of various lung adenocarcinoma cell lines and xenograft tumor models.

Methods *In vitro*, H2228, H1993, and A549 cells were treated with crizotinib. The inhibition of proliferation was quantitated by a 3-(4, 5-dimethylthiazol-2-yl)-2, 5-diphenyltetrazolium bromide (MTT) assay. Apoptosis was quantified by flow cytometry. Expression of key proteins of the HGF/c-Met signaling pathway was examined by western blotting. *In vivo*, H1993 and A549 tumor cell xenograft models were established. Immunohistochemical analysis was used to determine protein expression of HGF and c-MET and the amount of phospho-c-MET (p-c-Met). Real-time quantitative polymerase chain reaction (PCR) was applied to examine the messenger RNA (mRNA) expression of c-MET and serine/ threonine protein kinase (AKT). The expression and activation of the key proteins were evaluated by western blotting.

Results *In vitro*, the growth of H1993, H2228, and A549 cells was inhibited after crizotinib treatment for 72 h. Apoptotic rates of H1993 and H2228 cells increased with the crizotinib concentration and exposure time. *In vivo*, the growth-inhibitory rate of crizotinib for H1993 xenografts was 72.3%. Positive expression rates of HGF and c-MET in H1993 xenografts were higher than those in A549 xenografts; the p-c-MET amount was the largest in H1993 xenograft control but the lowest in the H1993 xenograft with crizotinib treatment. The mRNA expression levels of c-MET and AKT in H1993 xenografts were higher than those of A549 xenografts. The protein levels of c-MET, AKT, and extracellular regulated protein kinases (ERK) in H1993 xenografts were higher than those in A549 xenografts; the p-AKT amount was higher in H1993 xenograft control than in A549 xenografts; the largest amount of p-c-MET was detected in H1993 xenograft control; the amount of p-ERK was the lowest in the H1993 xenograft with crizotinib treatment.

Conclusion The HGF/c-Met signaling pathway may mediate crizotinib-induced apoptosis and inhibition of proliferation of lung adenocarcinoma cells.

Received: 4 December 2016
Revised: 25 December 2016
Accepted: 9 February 2017

Key words: HGF/c-MET signaling pathway; H1993 cells; H2228 cells; crizotinib; apoptosis

Lung cancer is the leading cause of cancer-related deaths worldwide, and nearly 80% of patients with non-small cell lung cancer (NSCLC) receive the diagnosis at an advanced stage. The efficacy of platinum-based doubled regimens is limited, with progression-free survival and median survival of only 4–5 months and 8–9 months, respectively. In recent years, precision medicine, which involves diagnosis and treatment based on a patient's biogenetic information, has been increasingly applied. In patients with NSCLC containing *EGFR* mutations or *ALK* rearrangements, targeted therapies represent the standard of care, with superior efficacy and improved

✉ Correspondence to: Xiangqun Song. E-mail: xiangquns@163.com
* Supported by grants from the National Natural Sciences Foundation of China (No. 81060188 and No. 81260351) and Guangxi Sciense & Technology Development Funds (No. 2015139 and No. 201017).

tolerability, compared with chemotherapy. These two genetic alterations are relatively common and are found in tumors of approximately 15% and 5% of patients with NSCLC, respectively. Extensive profiling efforts have identified molecular drivers in subsets of NSCLC.

The proto-oncogene *c-Met* encodes receptor tyrosine kinase *c-Met*, which belongs to the class of transmembrane receptors with autophosphorylation activity [1]. After a specific natural ligand called hepatocyte growth factor (HGF) binds to c-Met's extracellular domain, *c-Met* can undergo dimerization and autophosphorylation and subsequently activate downstream signaling pathways such as PI3K/AKT, Ras-Rac/Rho, MAPK/MAP, and STAT3/survivin signaling cascades [2]. In some cases, abnormal activation of HGF/c-Met signaling contributes to oncogenesis and tumor progression in a variety of cancers and promotes invasiveness that is strongly linked to tumor metastasis [3]. The most common aberrant types of c-Met genes include *c-Met* point mutations and amplification. *c-Met* amplification is present in tumors of approximately 2.2% and 5% of NSCLC patients untreated or with failed treatment with EGFR tyrosine kinase inhibitors (EGFR-TKIs), respectively [4]. Preclinical analysis has shown that growth and survival of lung cancer cell lines with *c-Met* primary amplification depend on activation of the HGF/c-Met signaling pathway [5]. Targeting *c-Met* may be a promising strategy for lung cancer treatment, but there are few relevant studies. Crizotinib (PF-02341066), an inhibitor of tyrosine kinase activity of *c-Met*, ALK, and ROS-1, has been shown to be effective in the treatment of patients with EML4-ALK- or ROS-1-positive NSCLC and was approved by the Food and Drug Administration in August 2011 and March 2016, respectively. NSCLC harboring strongly amplified *c-Met* or *c-Met* exon 14 alterations may represent independent c-Met phenotypes and responses to crizotinib [6–7]. National Comprehensive Cancer Network (NCCN) Guideline Version 2.2016 NSCLC expanded the indications for the strong *c-Met* amplification or *c-Met* exon 14 skipping mutation and ROS-1 rearrangements. Nonetheless, the role of the HGF/c-Met signaling pathway in crizotinib-induced apoptosis in NSCLC with *c-Met* amplification has yet to be determined.

In this study, we evaluated the role of the HGF/c-Met signaling pathway in crizotinib-induced apoptosis of various lung adenocarcinoma cell lines and xenograft tumor models and analyzed the possible regulatory mechanisms with the goal of providing a scientific basis for crizotinib use in the treatment of primary or secondary *c-Met* amplification-positive NSCLC as well as experimental data on its efficacy and safety.

Materials and methods

Materials

Cell lines

c-Met amplification-positive human lung adenocarcinoma cell line H1999 and E*ML4-ALK*-positive human lung adenocarcinoma cell line H2228 (*ALK* rearrangement variant type V3) were acquired from the American Type Culture Collection. The A549 cell line was provided by the Experimental Center of The Affiliated Tumor Hospital of Guangxi Medical University.

Mice

Male specific-pathogen-free (SPF), 3- to 5-week-old, BALB/C nude mice (18–22 g, n = 40) were purchased from the Animal Experimental Center of Guangxi Medical University (Permission No. for Laboratory Animals: SYXK GUI 2014-0002). The animals were housed in autoclaved Micro-Isolater clear plastic cages, with a ventilation rate of 10 to 15 air changes per hour, at 20°C, 50% relative humidity, and in a light/dark cycle of 12/12 h, with free access to standard rodent food pellets and water. All animal experimentation was performed according to institutional guidelines and with approval of a local institutional review board.

Reagents and instruments

Crizotinib was acquired from Cell Signaling Technology (USA). The RPMI-1640 medium, fetal bovine serum (FBS), and trypsin were purchased from Gibco (USA). A 3-(4, 5-dimethylthiazol-2-yl)-2, 5-diphenyltetrazolium bromide (MTT) solution and dimethyl sulfoxide (DMSO) were purchased from Amresco (USA). The Annexin-V-PE/7AAD apoptosis detection kit and the Bicinchoninic acid (BCA) kit were purchased from BD (USA) and Merck (China), respectively. The SP Immunohistochemical (IHC) Kit was acquired from Boosen Biological Technology (China). Diaminobenzidine (DAB) was purchased from Hill-bridge Company (China). The Total RNA Small Amount Preparation Kit was purchased from Axygen Corelle Life Science Company (China). The cDNA Synthesis Kit was acquired from Bao Biological Engineering Company (China), and the Quantitative PCR Kit and Phosphatase Inhibitors Cocktail Tablets were purchased from Roche (Switzerland). The BCA Protein Assay Kit was acquired from Beyotime Biotech Company (China). HGF, c-MET, phosphorylated c-MET (p-c-MET; Tyr1003), AKT, p-AKT (Ser473), ERK, p-ERK (Thr202/Thr204), and β-actin antigen reagents and antibodies were purchased from Cell Signaling Technology (USA). Fluorescence type II antigen and antibody were purchased from Poly Biological Technology (China). Supersensitive ECL Chemical Luminescence Substrate was purchased from Boster Biological Engineering Company (China). The quantitative PCR instrument was acquired from Eppendorf (Germany). The JY-ECPT3000 electrophoresis

device was purchased from Liuyi instrument factory (China). Western blot equipment and a type 170-8170 protein imaging instrument were acquired from Bio-Rad Company (USA).

Methods

Cell culture

Cells were cultured in the RPMI 1640 medium supplemented with 10% of FBS at 37°C in a humidified atmosphere containing 5% of CO_2. The culture medium was removed every 2–3 days, and 1–2 mL of a trypsin-ethylene diamine tetraacetic acid (EDTA) solution was added. The flask was allowed to incubate at room temperature until the cells got detached. A fresh culture medium was added, and the solution was aspirated and dispensed into new culture flasks.

The MTT assay

Attached H1993, H2228, and A549 cells in culture were digested with 0.25% trypsin until they got detached. The cells were centrifuged, the supernatant was discarded, and the cells were resuspended in the complete growth medium. After the cell density was adjusted to 800 per mL, the cells were seeded in 96-well plates at 100 μL/well, and incubated overnight at 37°C and 5% CO_2. The cells were then exposed to 10, 30, 90, 270, or 810 nM crizotinib for 72 h. Absorbance at 490 nm (A490) was measured on a Multiskan Spectrum spectrophotometer. Each assay consisted of six replicate wells and was repeated at least three times independently. Inhibition of cell proliferation was calculated as follows: [1 - (A_{490} of experimental group -A_{490} of blank group) (A_{490} of control group - optical density of blank group)] × 100%.

Flow cytometric analysis of the effect of crizotinib on apoptosis

Attached H1993, H2228, and A549 cells in culture were digested with 0.25% trypsin and centrifuged. The supernatant was discarded, and the cells were resuspended in the complete growth medium. The cell densities were adjusted to 3×10^5/mL, 6×10^5/mL, and 10^6/mL, respectively, and the cells were seeded in 6-well plates at 2 mL/well. Crizotinib at 200, 300, and 300 nM was added to the medium of H1993, H2228, and A549 cells, respectively. The cells were cultured for 24, 48, or 72 h, and were harvested by incubation with 0.25% trypsin without EDTA, washed with phosphate-buffered saline (PBS), and centrifuged at 300 × *g* for 5 min. The cell pellets were resuspended in 100 μL of the Annexin-V-PE/7AAD labeling solution, and incubated for 15 min at room temperature in the dark. After addition of propidium iodide (PI) and fluorescein from the isothiocyanate (V-PE/7AAD) staining kit, the cells were resuspended in 400 μl of the Annexin-V-PE/7AAD labeling solution and then analyzed for fluorescence by flow cytometry.

Western blot analysis

Cells were washed twice with ice-cold PBS and then lysed in a solution containing phosphatase inhibitors cocktail tablets, phenylmethanesulfonyl fluoride (PMSF), and RIPA Lysis Buffer (100 mM), according to the manufacturer's protocol. The protein concentration in the cell lysates was measured using the BCA kit, and equal amounts of protein were subjected to sodium dodecyl sulfate polyacrylamide gel electrophoresis (SDS-PAGE) in an 8% or 10% gel. β-Actin served as an internal reference. The separated proteins were transferred to polyvinylidene fluoride (PVDF) membranes, which were then exposed to 5% bovine serum albumin (BSA) in PBS for 2 h at room temperature before overnight incubation at 4°C with primary antibodies. The membranes were incubated for 1 hour at room temperature with horseradish peroxidase-conjugated goat antibodies to rabbit, horse, or mouse IgG. According to the manufacturer's protocols, the c-MET antibody, p-c-MET (Tyr1003) antibody, AKT antibody, p-AKT (Ser473) antibody, ERK antibody, p-ERK (Thr202/Thr204) antibody, and the β-actin antibody were used at 1:1000, 1:1000, 1:2000, 1:2000, 1:1000, 1:2000, and 1:1000 dilutions, respectively. The membranes were incubated for 1 h at room temperature with horseradish peroxidase-conjugated goat antibodies to rabbit or horse antibodies to mouse IgGThe membranes were incubated for 1 h at room temperature with horseradish peroxidase-conjugated goat antibodies to rabbit or horse antibodies to mouse IgG, which were used at a 1:2000 dilution.

Animal grouping and treatment

Forty SPF BALB/C nude mice were randomly allocated to 5 groups on average: H1993 xenograft control (Group A), H1993 xenograft with crizotinib (Group B), A549 xenograft control (Group C), A549 xenograft with crizotinib (Group D), and healthy control (Group E). For the tumor inoculation model, subcutaneous tissue of the left axillary region from BALB/C mice was injected with the H1993 or A549 cell line at a concentration of 5×10^7 cells per 100–150 μL. The animal models were regarded as successful when the tumor size reached 200–600 mm^3 (day 0) in each mouse. Treatment groups consisted of control and crizotinib-administered (50 mg/kg of body weight, which was dissolved in 0.2 mL of distilled water) mice. Crizotinib was administered by oral gavage daily for 14 days; control animals received 0.2 mL of distilled water as vehicle. Weight, food intake, and tumor size of the mice were measured every 3 days from the day of crizotinib administration. Tumor volume was determined by caliper measurements of tumor length (L) and width (W) according to the formula $L \times W^2/2$. Tumor growth curves and inhibition rates were calculated. Euthanasia by cervical dislocation was performed 24 h after the last drug administration, and tumors were completely excised

for further analysis. Percentages of inhibition of tumor volume were measured on the final day of the experiment for drug-treated versus vehicle-treated mice and were calculated as follows: [($Control_{final\ day}$ - $Treated_{final\ day}$) / $Control_{final\ day}$].

IHC analysis

Sections of 4-μm thickness cut from formalin-fixed paraffin-embedded tissue blocks were deparaffinized in xylene and rehydrated in a graded series of aqueous ethanol solutions. Levels of HGF, c-MET, and p-c-MET in tumor tissues were measured by means of the SP kit. IHC staining results were assessed using the criteria of Fromowitz semiquantitative classification, where the total score = staining intensity score + proportion of positive cells score. Staining intensity was scored based on membrane staining intensity: 0 = no staining, 1 = faint yellow, 2 = pale brown, and 3 = dark brown. The proportions of positive cells were scored as follows: < 5% for score = 0, 5%–25% for score = 1, 26%–50% for score = 2, 51%–75% for score = 3, and > 75% for score = 4. The total score < 2 was defined as negative (-), 2–3 as weakly positive (+), 4–5 as moderately positive (++), and 6–7 as strongly positive (+++). Low and high expression were designated as "-" to + and ++ to +++, respectively.

Real-time quantitative polymerase chain reaction (RT-qPCR)

Total RNA was extracted from snap-frozen samples by means of the TRIzol Reagent (Invitrogen, USA). Complementary DNA was synthesized from 500 ng of total RNA using the cDNA Synthesis Kit (Bao Biological Engineering Company, China). The gene-specific primers for c-MET and AKT are listed in Table 1. The primers were synthesized by the Hua Da gene Polytron Technology Company (China). For normalization of the RNA quality and quantity, expression of β-actin in each sample was quantified. Messenger RNA (mRNA) expression of c-MET and AKT was determined using the SYBR Green-Based RT-PCR Kit and a quantitative RT-PCR system (Germany) under the following conditions: an initial denatur¬ation step of 95°C for 10 min, followed by 40 amplifica¬tion cycles involving denaturation at 95°C for 15 sec and annealing with elongation at 60°C for 1 min. Signals with a (maximal curvature) threshold cycle (Cq) value of > 35 were assumed to indicate no transcription of the target gene. A melting-curve analysis was conducted to monitor PCR product purity, and relative gene expression data were analyzed by the $2^{-\Delta\Delta Ct}$ method: $\Delta\Delta Cq = (Cq_{target\ gene} - Cq_{internal\ control})_{testing\ sample} - (Cq_{target\ gene} - Cq_{internal\ control})_{standard\ sample}$. One randomly selected sample served as a reference sample to calculate the relative quantity value.

Table 1 Dose-volume constraints for PTV and OARs

Gene	Sequence (5`-3`)	Primer lengt (bp)	Annealing temperature (℃)
β-actin	Forward CCTCGCCTTTGCCGATCC	102	60
	Reverse TTGCACATGCCGGAGCC	102	60
AKT	Forward TGGACGATAGCTTGGAGGGA	241	61
	Reverse ATTGTTCTGAGGGCTGAGGC	241	61
c-MET	Forward GAGAAGACTCCTACAACCCGAAT	287	59
	Reverse AGTACTAGCACTATGATGTCTCCC	287	59

Western blot analysis

Total protein was extracted from transplanted tumor tissue by means of a solution containing phosphatase inhibitors cocktail tablets, PMSF, and RIPA Lysis Buffer (100 mM), according to the manufacturer's protocol. The total amount of protein was determined with the BCA Kit. Western blot procedures were described above.

Statistical analysis

Quantitative data are shown as mean ± standard deviation. Two sets of data were analyzed using unpaired two-tailed Student's *t* test. One-way ANOVA was applied when homogeneity of variance assumptions were satisfied (multiple comparisons between groups were conducted using SNK analysis of variance); otherwise, the Kruskal-Wallis *H* test was used (multiple comparisons between groups were performed by Kruskal-Wallis analysis of variance). The data were analyzed using the SPSS software, version 19.0, and $P < 0.05$ was considered to indicate statistical significance. Probit regression analysis was used to calculate IC_{50} with a 95% confidence interval (CI).

Results

Effects of crizotinib on H1993, H2228, and A549 cells growth

The IC_{50} values of crizotinib for H1993 and H2228 cells were found to be 179 and 335 nM, respectively. A549 cells were nearly insensitive to crizotinib at concentrations below ~10 nM, and the IC_{50} value for A549 cells could not be determined even after crizotinib administration at a concentration of 10,000 nM (Fig. 1). Crizotinib inhibited the growth and proliferation of H1993 and H2228 cells in a concentration-dependent manner.

Apoptotic effects of crizotinib on H1993, H2228, and A549 cells

Crizotinib induced apoptosis of H1993 and H2228 cells, but not in A549 cells ($P < 0.05$). At 179 nM crizotinib,

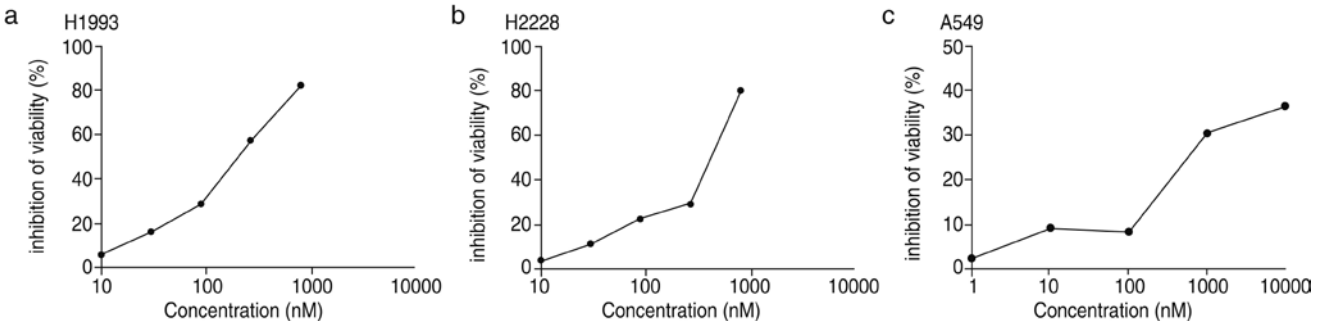

Fig. 1 Crizotinib inhibits the viability of 3 cell lines of NSCLC. H1993, H2228 and A549 cells were treated with crizotinib at different concentrations for 72 h. Percent inhibition was determined by the MTT assay. (a) The IC_{50} values of crizotinib for H1993 cells were found to be 179 nM; (b) The IC_{50} values of crizotinib for H2228 cells were found to be 335 nM; (c) A549 cells were nearly insensitive to crizotinib at concentrations below ~10 nM, and the IC_{50} value for A549 cells could not be determined even after crizotinib administration at a concentration of 10,000 nM.

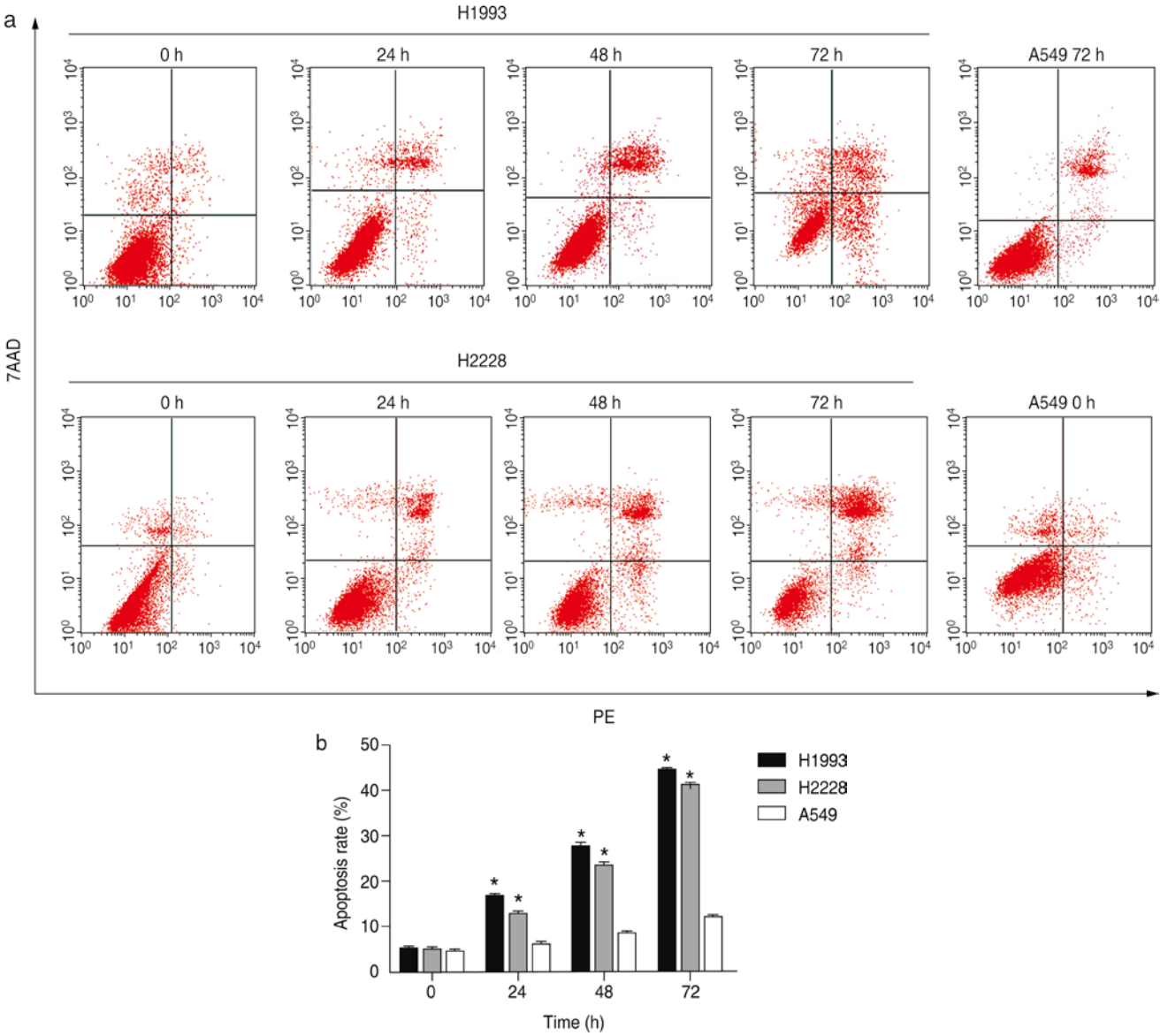

Fig. 2 Cell apoptosis rates of H1993, H2228 and A549 after treated with crizotinib at different times (0 h, 24 h, 48 h, 72 h). (a) Crizotinib induced apoptosis of H1993 and H2228 cells, but not in A549 cells ($P < 0.05$); (b) At 179 nM crizotinib, the apoptotic fractions of H1993 cells at 24, 48, and 72 h were 15.3% ± 2.1%, 27.2% ± 1.6%, and 46.5% ± 1.8%, respectively, while that of A549 cells at 72 h was 15.64% ± 0.61%. At 335 nM, the apoptotic fractions of H2228 cells at 24, 48, and 72 h were 13.7% ± 0.8%, 25.3% ± 1.6%, and 43.5% ± 3.2%, respectively.

the apoptotic fractions of H1993 cells at 24, 48, and 72 h were 15.3% ± 2.1%, 27.2% ± 1.6%, and 46.5% ± 1.8%, respectively, while that of A549 cells at 72 h was 15.64% ± 0.61%. At 335 nM, the apoptotic fractions of H2228 cells at 24, 48, and 72 h were 13.7% ± 0.8%, 25.3% ± 1.6%, and 43.5% ± 3.2%, respectively (Fig. 2). Crizotinib induced apoptosis of H1993 and H2228 cells in a time-dependent manner.

Effects of crizotinib on the expression of apoptosis-related proteins in the HGF/c-Met signaling pathway

The total amount of c-MET (c-MET plus p-c-MET) in H1993 cells treated with 200 nM crizotinib decreased as compared with untreated H1993 cells and with A549 cells. A significant decrease in the amounts of p-AKT, p-ERK, and p-c-MET was observed at 24 h after crizotinib treatment. Crizotinib decreased the amounts of p-AKT, p-ERK, and p-c-MET in H1993 cells in a time-dependent manner. The level of p-c-MET at 72 h was the lowest, as compared with that of p-AKT and p-ERK. In H2228 cells, expression levels of c-MET, AKT, and ERK after 300 nM crizotinib treatment were not detectable as compared with untreated cells. Nevertheless, significant decreases in the amounts of p-AKT, p-ERK, and p-c-MET were observed after 48 h. Minimal levels of those phospho-proteins were observed after 72 h. Amounts of c-MET, p-c-MET, AKT, p-AKT, ERK, and p-ERK in A549 cells showed no changes after treatment with 300 nM crizotinib (Fig. 3).

Viability of crizotinib-treated NSCLC nude mice

Average daily food intake and body weight before and after crizotinib administration in NSCLC nude mice were shown in Fig. 4. Compared with Group E, the decrease in daily food intake that occurred in the other groups was statistically significant ($P < 0.05$). The largest decrease was observed in Group A. There was no significant difference in daily food intake between Groups C and D ($P > 0.05$). As to body weight, increases were detected in Group B compared with Groups A, C, and D ($P < 0.001$). Only slow weight gains were observed in Groups A, C, and D

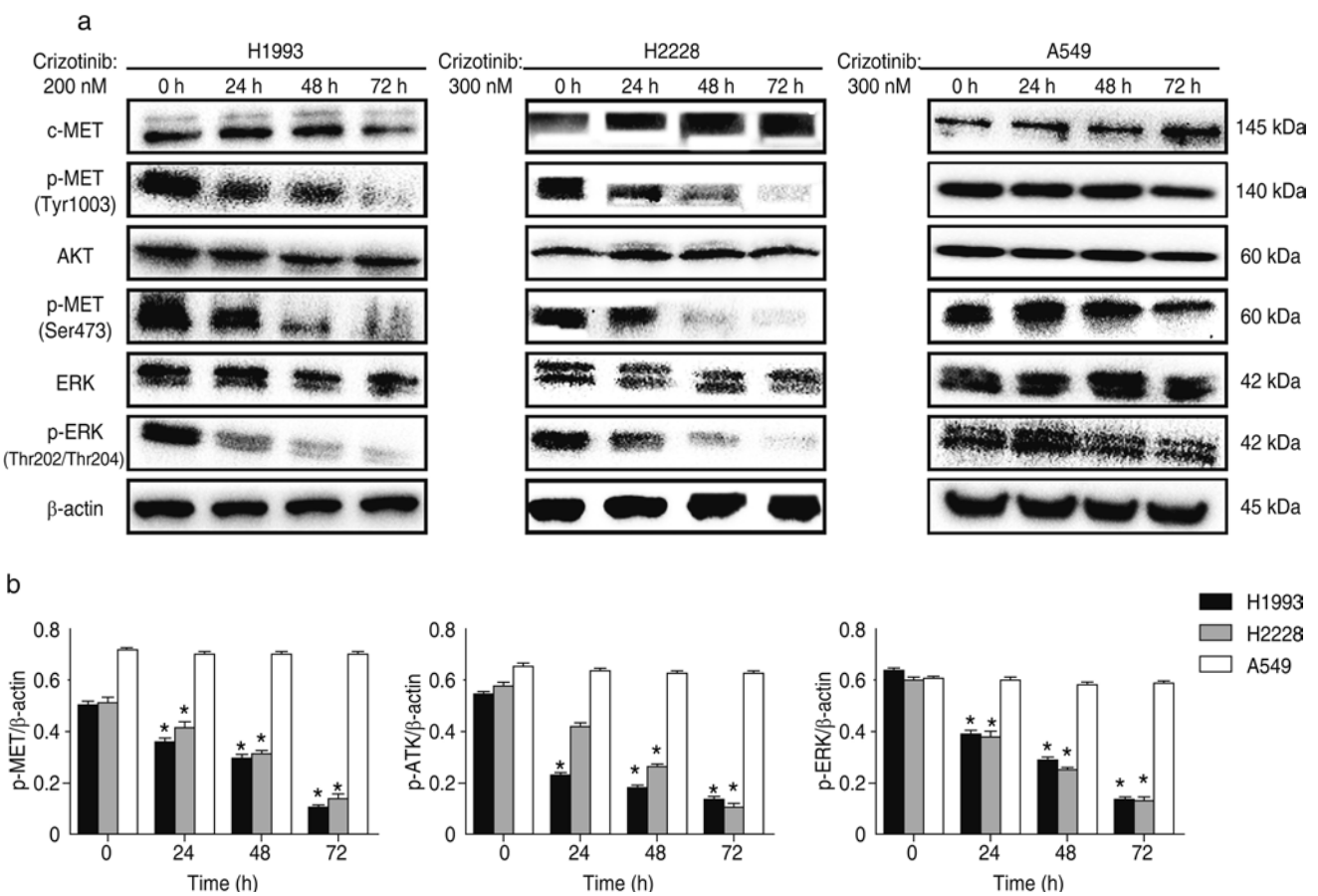

Fig. 3 Effect of crizotinib on expression of proteins in the 3 cell lines. (a) Protein levels in the 3 cell lines treated with crizotinib at different time-points (24 h, 48 h, 72 h) determined by Western blot; (b) Represents the relative expression of p-MET, p-AKT and p-ERK in 3 cells. n=3. *$P < 0.05$ compared with the control group (0 h).

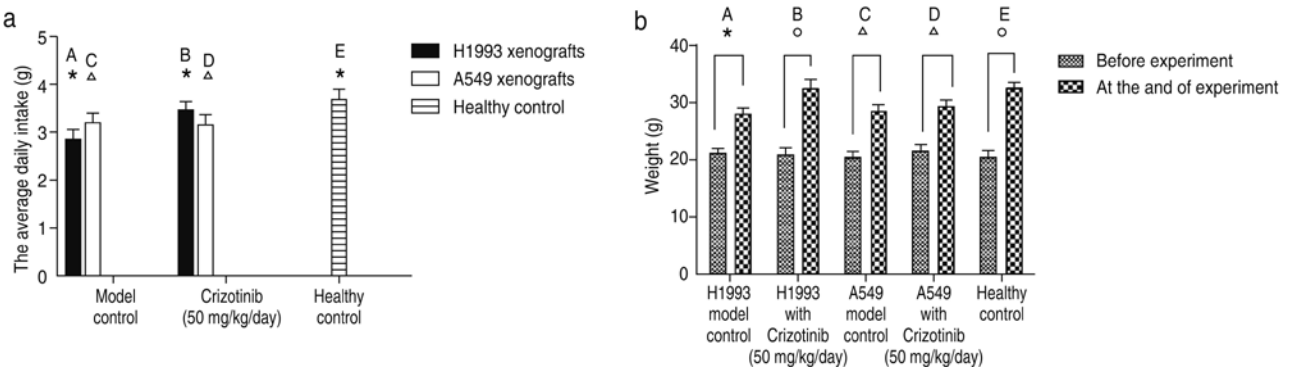

Fig. 4 Effects of crizotinib on life status of NSCLC xenograft tumor models. (a) Compared with other groups $^{*}P < 0.05$, compared with other groups except Group C or Group D $^{\triangle}P < 0.05$; (b) Compared with other groups $^{*}P < 0.001$, compared with other groups except Group C or Group D $^{\triangle}P < 0.001$, compared with other groups except Group B or Group E $^{\circ}P < 0.001$.

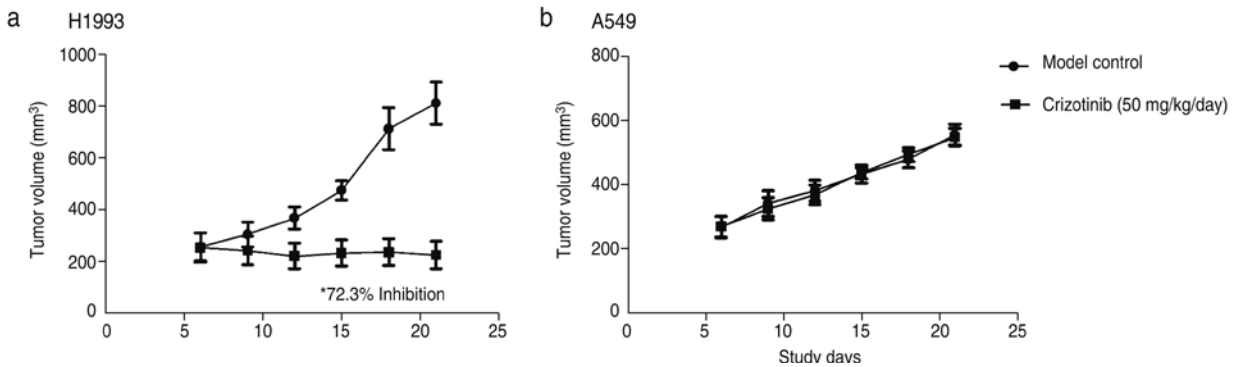

Fig. 5 NSCLC xenografts tumor size-time diagram. (a) The rate of inhibition of tumor volume for H1993 cells (in xenograft nude mice) by crizotinib was 72.3%, which is significantly higher than that in the control group ($P < 0.01$); (b) The inhibition of tumor volume of A549 cells in xenograft mice was only 1.3%, which is not different from that of the control group ($P > 0.05$).

compared with Group E ($P < 0.001$), with a remarkable difference for Group A. The results indicated that quality of life was better in the *c-Met* amplification NSCLC nude mice model and could be improved by treatment with crizotinib.

The tumor volume in NSCLC nude mice

The rate of inhibition of tumor volume for H1993 cells (in xenograft nude mice) by crizotinib was 72.3%, which is significantly higher than that in the control group ($P < 0.01$). The inhibition of tumor volume of A549 cells in xenograft mice was only 1.3%, which is not different from that of the control group ($P > 0.05$; Fig. 5). The results show that crizotinib exerts its growth inhibition on *c-Met* amplification-positive but not-negative NSCLC.

Amounts of HGF, c-MET, and p-c-MET in xenografts according to IHC analysis

The amounts of HGF, c-MET, and p-c-MET in 32 xenografts were determined by IHC analysis. The results showed that HGF is mainly located in the cytoplasm and the nucleus of tumor cells, and shows varying staining intensity. Positive expression of HGF in Groups A and B was higher than that of Groups C and D, but the differences were not statistically significant ($P > 0.05$). c-MET and p-c-MET were mainly located in the cytoplasm. Expression of c-MET in Groups A and B was also higher than that in Groups C and D, and the differences were statistically significant ($P < 0.0001$). The amount of p-c-MET in Group A was significantly higher than that in the other groups ($P < 0.0001$), while in group B, the amount of p-c-MET was the lowest. There were no differences in amounts of p-c-MET between Groups C and D (Fig. 6). The

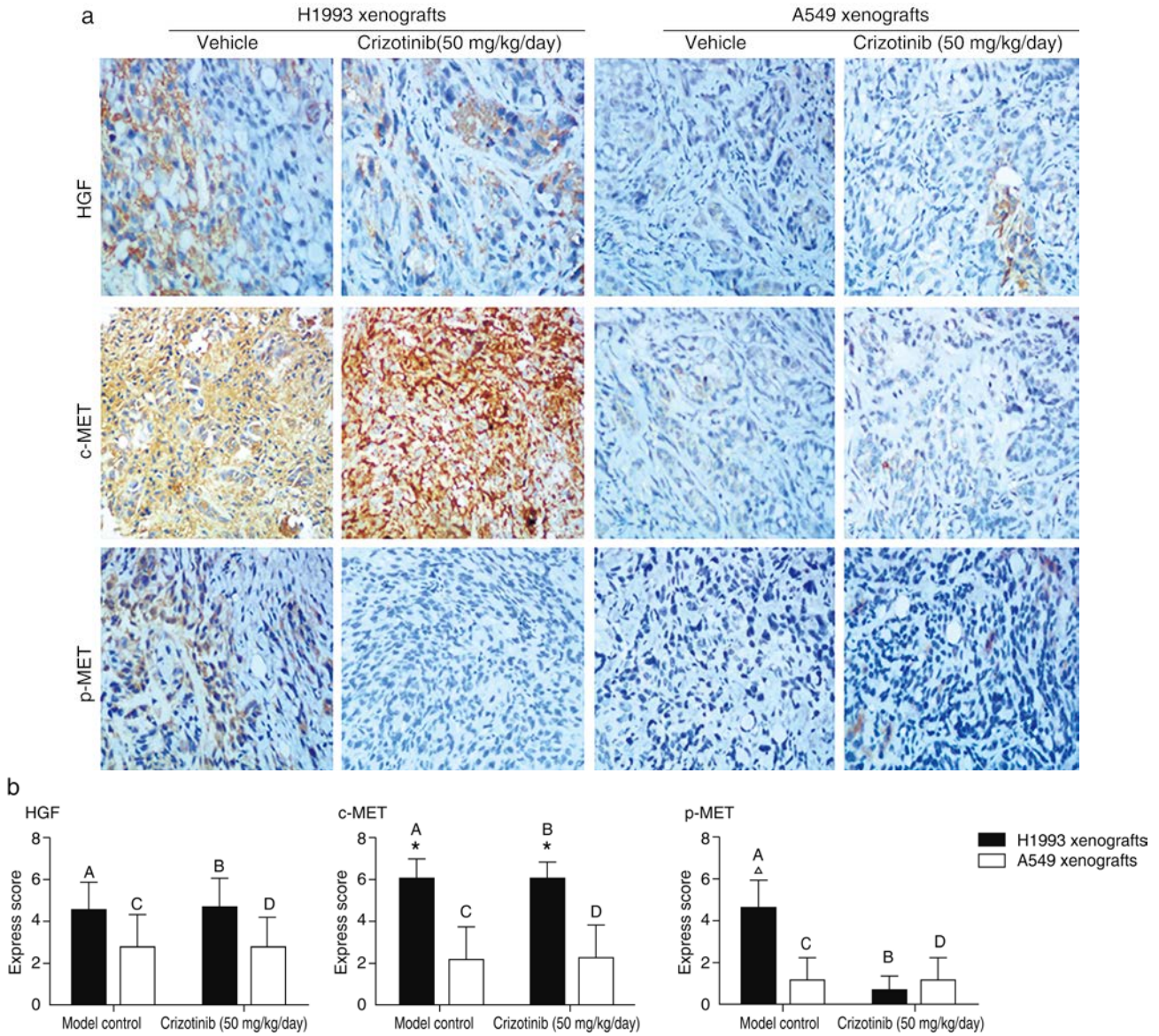

Fig. 6 Expression of HGF, c-MET, and p-MET in tumor tissues of NSCLC xenografts. (a) Original magnification×100; (b) *n*=8. Compared with other groups $^{\triangle}P < 0.0001$, compared with Group C and Group D $^{*}P < 0.0001$.

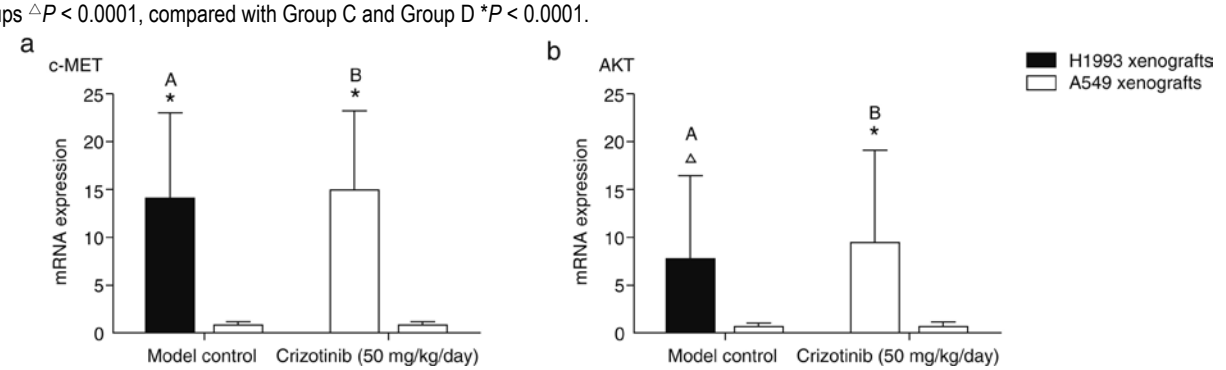

Fig. 7 Expression of c-MET, AKT mRNA in tumor tissues of NSCLC xenografts. (a)The mRNA expression of c-MET in Groups A and B were higher than that in Groups C and D, with statistical significance ($P < 0.001$, $P < 0.001$, respectively). In Group B showed no significant differences from Group A ($P > 0.05$). No differences between Groups C and D were detected ($P > 0.05$); (b)The mRNA expression of AKT in Groups A and B were higher than that in Groups C and D, with statistical significance ($P < 0.05$, $P < 0.001$, respectively). In Group B showed no significant differences from Group A ($P > 0.05$). No differences between Groups C and D were detected ($P > 0.05$).

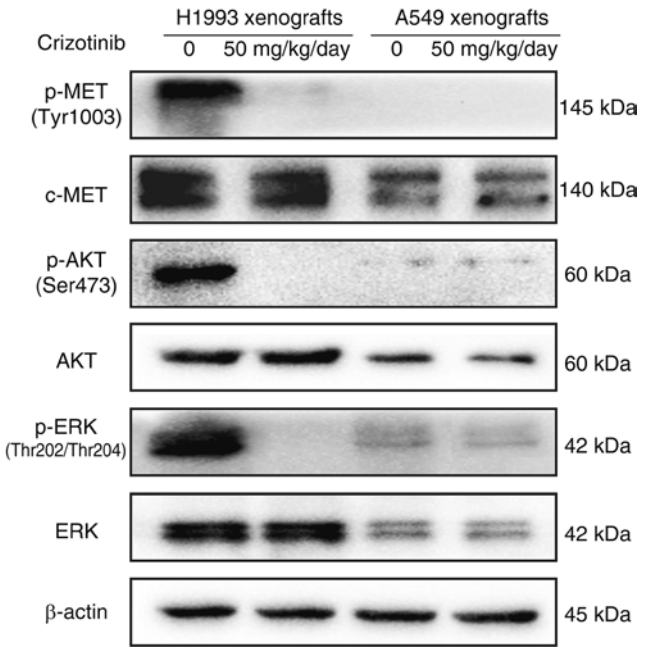

Fig. 8 Effect of crizotinib on expression of proteins in tumor tissues of NSCLC xenografts.

results show that the level of expression of HGF is unrelated to the status of *c-Met* amplification and the use of crizotinib. High expression of c-MET in H1993 cells can be inhibited by crizotinib, and this effect may contribute to the suppression of the growth of tumor tissue in nude mice harboring *c-Met* amplification in the xenograft.

Influence of crizotinib on mRNA expression of c-MET and AKT

The mRNA expression of c-MET and AKT in Groups A and B were higher than that in Groups C and D, with statistical significance ($P < 0.001$, $P < 0.001$, $P < 0.05$, and $P < 0.001$, respectively). The mRNA expression of c-MET and AKT in Group B showed no significant differences from Group A ($P > 0.05$). No differences between Groups C and D were detected ($P > 0.05$; Fig. 7). These results show that crizotinib had little or no effect on the mRNA expression of c-MET and AKT.

Influence of crizotinib on the expression of c-MET and related proteins of the Akt/Erk signaling pathway

Expression of c-MET, AKT, and ERK in xenografts was significantly higher in Groups A and B than in Groups C and D ($P < 0.001$, $P < 0.05$, and $P < 0.01$, respectively). Nonetheless, the difference between Groups A and B was not significant ($P > 0.05$). The amount of p-c-MET was higher in xenografts of Group A in comparison with the other groups, with statistical significance ($P < 0.05$). The expression of p-AKT in Group A was higher than that in the other groups ($P < 0.001$, $P < 0.05$, and $P < 0.05$, respectively). Compared with the other groups, the lowest expression of p-ERK was detected in Group B ($P < 0.01$; Fig. 8 and Table 2). The results indicate that crizotinib inhibits the growth of tumor tissue in H1993 xenografts by downregulating the phosphorylation of c-MET and related downstream proteins of the Akt/Erk signaling pathway.

Discussion

c-MET, which is encoded by the *c-Met* proto-oncogene, can be autophosphorylated on its intracellular tyrosine residues after binding its natural ligand HGF, and the phosphorylated protein subsequently activates a variety of key downstream signaling cascades, including the PI3K/Akt, Ras/MAPK, and survivin/STAT3 pathways [8]. Under normal conditions, activation of the HGF/c-Met pathway plays an essential regulatory role in embryonic development and tissue repair. In contrast, disturbances or overactivation of the HGF/c-Met pathway can promote cell proliferation, increase angiogenesis, enhance tumor invasion and metastasis, and decrease apoptosis [9].

Preclinical studies suggest that growth and survival of lung cancer cells harboring *c-Met* amplification depend on persistent activation of the HGF/c-Met pathway [5]. Clinically, secondary amplification of the *c-Met* may be involved in the development of EGFR-TKIs resistance [10]. Pao *et al* [11] proposed that cancer cells can activate the *c-Met* signaling pathway for sustained survival after blockade of the EGFR signaling pathway. The main cause of *c-Met* amplification is the breakage-fusion-bridge mechanism [12]. Based on the ratio of *c-Met* to centromere of chromosome 7, the degree of *c-Met* amplification is subdivided into 3 categories: 1.8–2.2 for

Table 2 Effects of crizotinib on indicated proteins expression in tumor tissues of NSCLC xenografts

Group	c-MET	p-MET	AKT	p-AKT	ERK	p-ERK
A	2.26 ± 0.45*	1.04 ± 0.30△	1.42 ± 0.36*	1.29 ± 0.30△	2.60 ± 0.90*	1.73 ± 1.58
B	2.24 ± 0.55*	0.25 ± 0.12	1.49 ± 0.41*	0.21 ± 0.10△	2.69 ± 0.85*	0.21 ± 0.09○
C	1.23 ± 0.28	0.36 ± 0.10	0.78 ± 0.16	0.55 ± 0.28	0.75 ± 0.21	0.77 ± 0.38
D	1.28 ± 0.31	0.35 ± 0.12	0.71 ± 0.17	0.68 ± 0.27	0.70 ± 0.20	0.82 ± 0.43

△, compared with each other groups: $P < 0.05$; *, compared with Group C and Group D : $P < 0.05$; ○, compared with other groups $P < 0.001$.

low amplification, 2.2–2.5 for moderate amplification, and ≥5 for a high degree of amplification. Commonly used in clinical trials involving a c-Met amplification-positive standard is a high *c-Met* gene copy number (mean ≥ 5 copies/cell) according to fluorescence *in situ* hybridization, as proposed by Cappuzzo in 2009 [13]. Amplification of *c-Met* leads to overexpression of receptor *c-MET*, which is susceptible to *c-MET* inhibitors. The development of crizotinib was originally aimed at *c-MET* (according to the eutectic structure of both PHA-665752 and the *c-MET* unphosphorylated kinase domain) via competitive inhibition of the binding and subsequent autophosphorylation of kinase *c-MET* and ATP hydrolysis.

Our findings also reveal the antiproliferative and proapoptotic effects of crizotinib on H1993 and H2228 cells. Inhibition by crizotinib is both time-dependent and concentration-dependent. Similar inhibition was not observed in A549 and crizotinib-untreated cells.

Akt, as a key molecule of the PI3K/Akt/mTOR signaling pathway, plays an important role by activating such molecules as mTOR and by phosphorylating such proteins as Bcl-2 and Fox, thus inhibiting apoptosis [14]. ERK is a downstream effector of the MAPK signaling pathway and can be activated by phosphorylation, and then p-ERK enters the nucleus to promote phosphorylation of transcription factor NF-κB and c-Myc and to enhance cell proliferation and to reverse proapoptotic effects of drugs [15]. The presence of p-AKT and p-ERK is viewed as the main sign of activation of the HGF/c-Met signaling pathway.

In this study, we evaluated the expression of c-MET, AKT, ERK, and their active forms of signaling proteins by western blotting and showed that the amounts of p-c-MET, p-AKT, and p-ERK in H1993 and H2228 cells are all decreased by crizotinib in a time-dependent manner. These results suggest that crizotinib inhibits activation of the Akt and Erk signaling pathways and downregulates the phosphorylation of AKT and ERK by decreasing c-MET activation (i.e., phosphorylation). These inhibitory effects promote apoptosis of tumor cells. This finding is consistent with the results of Junko and Akihiro [16,17].

In addition, we observed that complete disappearance of p-c-MET occurred at 72 h after crizotinib administration, whereas the expression of the downstream signaling proteins p-AKT and p-ERK was not suppressed completely. Thus, we assume that other pathways may be involved in activating the AKT and ERK downstream signaling pathways. It has been proven that c-MET inhibits apoptosis of lung cancer cells via activation of the p53 signaling pathway [18]. Belal *et al* [19] reported cross-talk between the c-Met and *EGFR* signaling pathways, which does not take place directly but is induced by Erk, c-Met, and other mediators. Blockage of the EGFR or Erk signaling pathways can decrease the expression and activation of c-MET in EGFR-mutant and wild-type NSCLC cells. In a phase I trial evaluating the safety and efficacy of crizotinib in advanced NSCLC with *c-Met* amplification (ClinicalTrials.gov NCT00585195), the effective rates of treatment in patients with low, moderate, and high *c-Met* amplification were 0%, 17%, 67%. A dose of crizotinib of 50 mg/kg of body weight daily was used in that trial and is similar to the dose used in the phase I clinical trial of crizotinib for the treatment of NSCLC patients with *ALK* fusion or *c-Met* amplification. In line with Tanizaki's results[16], our findings indicate that crizotinib significantly improves quality of life of the nude mice with *c-Met* amplification in the NSCLC xenograft. Food intake of the mice with a *c-Met* amplification-positive NSCLC xenograft was significantly decreased compared with that of the control groups. Of note, the weight loss that occurred in the *c-Met* amplification-positive model did not reach statistical significance, suggesting that known adverse effects of crizotinib such as nausea, vomiting, diarrhea, constipation, and other gastrointestinal symptoms were mild, and crizotinib was well tolerated. The general health condition of our mouse models of *c-Met* amplification-positive NSCLC was worse than that in the blank control group because of rapid proliferation of tumor cells, suggesting that growth and survival of tumor cells harboring *c-Met* amplification may depend on sustained activation of the HGF/c-Met signaling pathway [20].

In addition, crizotinib can effectively suppress the tumor growth of H1993 cell xenografts in nude mice by inhibiting tyrosine kinases of the HGF/c-Met pathway. Similar results were not observed in the A549 cell xenograft models. Zou *et al* [21] found that crizotinib exerts its inhibition on c-MET tyrosine kinase activity in animal models of xenografts with *c-Met* amplification (gastric cancer, NSCLC, kidney, and prostate cancer cells), thus inducing apoptosis and attenuating ERK phosphorylation of the downstream AKT and MAPK pathways; this effect is similar to inhibition of the tyrosine kinase of *ALK* fusion variants under the influence of crizotinib. Our findings also show that crizotinib decreases the amounts of p-AKT and p-ERK by inhibiting c-MET phosphorylation instead of inhibiting expression of AKT and ERK during its *in vivo* antitumor action.

Other related studies show that strong phosphorylation of c-MET detected in H1993 cells may not be caused by activation by its ligand HGF. The c-Met knockdown by means of short hairpin RNA (shRNA) results in significant morphological changes of H1993 cells, whereas the proliferation of A549 cells is not inhibited by c-Met shRNA [22]. Our findings reveal that expression of HGF is not strongly related to *c-Met* status and crizotinib use. High expression of c-MET in c-Met amplification-

positive lung adenocarcinoma cells also indicates that activation of the c-Met signaling pathway is necessary for the survival of NSCLC.

It should be noted that in this study, we chose cell lines without *ALK* rearrangements for pharmacological experiments with c-MET. Nonetheless, owing to the expression of wild-type *ALK* gene in the selected cells, the pharmacological activities of crizotinib via ALK cannot be ruled out. Patients with advanced NSCLC with concomitant *EGFR* mutation and c-MET overexpression have significantly lower response rates to EGFR-TKIs, indicating that c-MET overexpression may cause intrinsic resistance to EGFR-TKIs. A combination of EGFR-TKIs and a c-MET inhibitor is a good strategy to overcome acquired resistance in patients with a c-MET–overexpressing tumor. One of the possible mechanisms of resistance may contribute to activities of both c-Met and EGFR signaling pathways.

Conclusion

This study shows that crizotinib, as a potent ATP-competitive inhibitor targeting kinase c-MET, can effectively inhibit the growth of H1993 and H2228 cells and the corresponding xenografts in nude mice. The inhibitory effect is directly related to the inhibition of c-MET phosphorylation and protein phosphorylation in its downstream pathway. Our findings provide the experimental basis and clinical reference for the use of c-MET inhibitors in the treatment of patients with NSCLC harboring *c-Met* amplification.

Conflicts of interest

The authors have no potential conflicts of interest.

References

1. Gherardi E, Birchmeier W, Birchmeier C, *et al*. Targeting MET in cancer: rationale and progress. Nat Rev Cancer, 2012, 12: 89–103.
2. Gibney GT, Aziz SA, Camp RL, *et al*. c-Met is a prognostic marker and potential therapeutic target in clear cell renal cell carcinoma. Ann Oncol, 2013, 24: 343–349.
3. Trovato M, Torre ML, Ragonese M, *et al*. HGF/c-met system targeting PI3K/AKT and STAT3/phosphorylated-STAT3 pathways in pituitary adenomas: an immunohistochemical characterization in view of targeted therapies. Endocrine, 2013, 44: 735–743.
4. Comprehensive molecular profiling of lung adenocarcinoma. Nature, 2014, 511: 543–550.
5. Lutterbach B, Zeng Q, Davis LJ, *et al*. Lung cancer cell lines harboring MET gene amplification are dependent on Met for growth and survival. Cancer Res, 2007, 67: 2081–2088.
6. Paik PK, Drilon A, Fan PD, *et al*. Response to MET inhibitors in patients with stage IV lung adenocarcinomas harboring MET mutations causing exon 14 skipping. Cancer Discov, 2015, 5: 842–849.
7. Caparica R, Yen CT, Coudry R, *et al*. Responses to crizotinib can occur in high-level MET-amplified non-small cell lung cancer independent of MET exon 14 alterations. J Thorac Oncol, 2017, 12: 141–144.
8. Gandhi L, Janne PA. Crizotinib for ALK-rearranged non-small cell lung cancer: a new targeted therapy for a new target. Clin Cancer Res, 2012, 18: 3737–3742.
9. Klapper LN, Kirschbaum MH, Sela M, *et al*. Biochemical and clinical implications of the ErbB/HER signaling network of growth factor receptors. Adv Cancer Res, 2000, 77: 25–79.
10. Engelman JA, Zejnullahu K, Mitsudomi T, *et al*. MET amplification leads to gefitinib resistance in lung cancer by activating ERBB3 signaling. Science, 2007, 316: 1039–1043.
11. Pao W, Chmielecki J. Rational, biologically based treatment of EGFR-mutant non-small-cell lung cancer. Nat Rev Cancer, 2010, 10: 760–774.
12. Smolen GA, Sordella R, Muir B, *et al*. Amplification of MET may identify a subset of cancers with extreme sensitivity to the selective tyrosine kinase inhibitor PHA-665752. Proc Natl Acad Sci USA, 2006, 103: 2316–2321.
13. Cappuzzo F, Marchetti A, Skokan M, *et al*. Increased MET gene copy number negatively affects survival of surgically resected non-small-cell lung cancer patients. J Clin Oncol, 2009, 27: 1667–1674.
14. Zimmer S, Kahl P, Buhl TM, *et al*. Epidermal growth factor receptor mutations in non-small cell lung cancer influence downstream Akt, MAPK and Stat3 signaling. J Cancer Res Clin Oncol, 2009, 135: 723–730.
15. Ehrenfeld P, Conejeros I, Pavicic MF, *et al*. Activation of kinin B1 receptor increases the release of metalloproteases-2 and -9 from both estrogen-sensitive and - insensitive breast cancer cells. Cancer Lett, 2011, 301: 106–118.
16. Tanizaki J, Okamoto I, Okamoto K, *et al*. MET tyrosine kinase inhibitor crizotinib (PF-02341066) shows differential antitumor effects in non-small cell lung cancer according to MET alterations. J Thorac Oncol, 2011, 6: 1624–1631.
17. Kogita A, Togashi Y, Hayashi H, *et al*. Activated MET acts as a salvage signal after treatment with alectinib, a selective ALK inhibitor, in ALK-positive non-small cell lung cancer. Int J Oncol, 2015, 46: 1025–1030.
18. Liu Y, Liu JH, Chai K, et al. Inhibition of c-Met promoted apoptosis, autophagy and loss of the mitochondrial transmembrane potential in oridonin-induced A549 lung cancer cells. J Pharm Pharmacol, 2013,65: 1622–1642.
19. Belalcazar A, Azana D, Perez CA, *et al*. Targeting the Met pathway in lung cancer. Expert Rev Anticancer Ther, 2012, 12: 519–528.
20. Timofeevski SL, McTigue MA, Ryan K, *et al*. Enzymatic characterization of c-Met receptor tyrosine kinase oncogenic mutants and kinetic studies with aminopyridine and triazolopyrazine inhibitors. Biochemistry, 2009, 48: 5339–5349.
21. Zou HY, Li Q, Lee JH, *et al*. An orally available small-molecule inhibitor of c-Met, PF-2341066, exhibits cytoreductive antitumor efficacy through antiproliferative and antiangiogenic mechanisms. Cancer Res, 2007, 67: 4408–4417.
22. Lutterbach B, Zeng Q, Davis LJ, *et al*. Lung cancer cell lines harboring MET gene amplification are dependent on Met for growth and survival. Cancer Res, 2007, 67: 2081–2088.

DOI 10.1007/s10330-016-0210-0
Cite this article as: Zhou SZ, Dong ZX, Lv JY, *et al*. The role of the HGF/c-Met signaling pathway in crizotinib-induced apoptosis in lung cancer with c-Met amplification. Oncol Transl Med, 2017, 3: 116–126.